The present situation and shifts observed in wetlands within the St. Lawrence Seaway region of Canada, utilizing imagery from the Landsat

Big Earth Data

ISSN: (Print) (Online) Journal homepage: www.tandfonline.com/journals/tbed20

The present situation and shifts observed in wetlands within the St. Lawrence Seaway region of Canada, utilizing imagery from the Landsat archive and the cloud-based platform Google Earth Engine

Meisam Amani, Mohammad Kakooei, Rebecca Warren, Sahel Mahdavi, Kevin Murnaghan, Arsalan Ghorbanian & Amin Naboureh

To cite this article: Meisam Amani, Mohammad Kakooei, Rebecca Warren, Sahel Mahdavi, Kevin Murnaghan, Arsalan Ghorbanian & Amin Naboureh (2025) The present situation and shifts observed in wetlands within the St. Lawrence Seaway region of Canada, utilizing imagery from the Landsat archive and the cloud-based platform Google Earth Engine, Big Earth Data, 9:1, 47-71, DOI: 10.1080/20964471.2025.2454044

To link to this article: https://doi.org/10.1080/20964471.2025.2454044

Published online: 14 Feb 2025.

BIG EARTH DATA
2025, VOL. 9, NO. 1, 47–71
https://doi.org/10.1080/20964471.2025.2454044

Taylor & Francis
Taylor & Francis Group

RESEARCH ARTICLE

OPEN ACCESS Check for updates

The present situation and shifts observed in wetlands within the St. Lawrence Seaway region of Canada, utilizing imagery from the Landsat archive and the cloud-based platform Google Earth Engine

Meisam Amani[a,b], Mohammad Kakooei[c], Rebecca Warren[d], Sahel Mahdavi[b], Kevin Murnaghan[a], Arsalan Ghorbanian[e] and Amin Naboureh[f]

[a]Canada Centre for Mapping and Earth Observation, Natural Resources Canada, Ottawa, ON, Canada; [b]Digital Environmental Group, WSP Canada Inc., Ottawa, ON, Canada; [c]Department of Computer Science, Chalmers University of Technology, Gothenburg, Sweden; [d]Digital Environmental Group, WSP Canada Inc., Edmonton, AB, Canada; [e]Department of Photogrammetry and Remote Sensing, Faculty of Geodesy and Geomatics Engineering, K. N. Toosi University of Technology, Tehran, Iran; [f]Research Center for Digital Mountain and Remote Sensing Application, Institute of Mountain Hazards and Environment, Chinese Academy of Sciences, Chengdu, China

ABSTRACT

This study examined wetland trends in the St. Lawrence Seaway (~500,000 km^2) in Canada over the past four decades. To this end, historical Landsat data within the Google Earth Engine (GEE) big geo data platform were processed. Reference samples were scrutinized using the Continuous Change Detection and Classification (CCDC) algorithm to identify spectrally unchanged samples. These spectrally unchanged samples were subsequently employed as training data within an object-based Random Forest (RF) model to generate wetland maps from 1984 to 2021. Subsequently, a change analysis was conducted to calculate the loss and gain of different wetland types. Overall, it was observed that approximately 45% (184,434 km^2) and 55% (220,778 km^2) of the entire study area are covered by wetland and non-wetland categories, respectively. It was also observed that 2.46% (12,495 km^2) of the study area was changed during 40 years. Overall, there was a decline in the Bog and Fen classes, while the Marsh, Swamp, Forest, Grassland/Shrubland, Cropland, and Barren classes had an increase. Finally, the wetland gain and loss were 6,793 km^2 and 5,701 km^2, respectively. This study demonstrated that the use of Landsat data, along with advanced machine learning and GEE, could provide valuable assistance for wetland classification and change studies.

ARTICLE HISTORY
Received 14 May 2024
Accepted 2 January 2025

KEYWORDS
Remote sensing; Google Earth Engine (GEE); cloud computing; satellite; change detection; continuous change detection and classification (CCDC); wetlands

CONTACT Meisam Amani meisam.amani@nrcan-rncan.gc.ca Digital Environmental Group, WSP Canada Inc., Ottawa, ON, Canada

1. Introduction

Wetlands play crucial roles in ecosystems, fulfilling various functions such as offering vital habitats for numerous plants and animals, preserving water quality, regulating floods, safeguarding shorelines, providing food and recreational activities for humans, and serving as a carbon sink (Mahdavi et al., 2018; Mitsch & Gosselink, 2007). However, approximately 54–57% of the Earth's original wetlands have vanished since 1700 AD, with the rate of loss accelerating by 3.7 times during the 20th and 21st centuries (Davidson, 2014). However, trends in wetland loss and alteration have continued to decline over time (Amani et al., 2021, 2022; Mirmazloumi et al., 2021). Hence, having baseline data regarding the widespread spatial distribution of wetlands is essential for monitoring these productive ecosystems, gathering insights into their historical conditions and shifts, and obtaining precise inputs for carbon budgeting, habitat preservation, biodiversity conservation, and resource management strategies.

Wetland mapping and change analysis can be either performed by in-situ measurements or remote sensing data. In-situ methods are not practically applicable to wetland monitoring over large areas due to significant time, cost, and safety risks. Moreover, wetland change detection over past periods is not feasible without field surveys conducted in those times. An alternative solution is to employ traditional aerial photo analysis, which usually provides accurate wetland mapping, though they are still expensive, cover relatively small areas, and are associated with human errors. Thus, the most practical and optimal method for detecting intra- and inter-annual as well as longer-term trends in wetland dynamics is through the utilization of spaceborne remote sensing systems. These systems offer up-to-date, archived, consistent, and multi-temporal datasets spanning several decades. Moreover, many satellites provide open-access datasets, which can effectively be used for wetland change detection in any region over the globe. The repeated broad coverages of these satellites also facilitate the development of national and international wetland inventories and policies (Jafarzadeh et al., 2022; Mahdavi et al., 2018; Mirmazloumi et al., 2021).

Multi-series satellite data are valuable resources for wetland change analysis in large areas over multiple decades. Yet, handling the vast volume of remote sensing data for such applications poses a challenge with traditional desktop processing and algorithms. Therefore, leveraging cutting-edge cloud computing platforms like Google Earth Engine (GEE) alongside advanced machine learning models becomes imperative.

GEE has considerably resolved the existing challenges of big geo data processing. The users have access to many types of satellite data, such as Landsat imagery, without any requirement to download and process the immense bulk of datasets within local computers. It also provides many pre-developed image processing, segmentation, and classification algorithms that can effectively be modified and applied to wetland mapping and change detection. More information about this platform can be found in (Amani et al., 2020; Gorelick et al., 2017; Tamiminia et al., 2020).

To date, several studies worldwide have employed Google Earth Engine (GEE) to analyze changes in wetlands. For example, Alonso et al. (2016) produced Normalized Differential Vegetation Index (NDVI) maps by utilizing time-series Landsat and Moderate Resolution Imaging Spectroradiometer (MODIS) data across a region in northwest Costa Rica. These maps were then used for wetland change analysis in GEE. They observed an

increase in the greenness of wetlands since 1986. Within-season variability of wetlands, which was related to seasonal precipitation dynamics, was also reported using MODIS-NDVI data. Moreover, Tang et al. (2016) evaluated the status of inundation of playa wetlands in Nebraska using several spectral indices derived from Landsat data between 1985 and 2015 in GEE. Their results showed that approximately 18% of the study area was inundated in the spring migratory season, and there were nearly 10,000 wetlands that were inundated at least once in either March or April from 1985 to 2015. Additionally, Mahdianpari et al. (2020) used 30 years of Landsat data in GEE to monitor wetland changes in Newfoundland, Canada. The authors reported that the Random Forest (RF) performed better than other classification algorithms. They also noted that wetland trends exhibited instability over the past three decades, primarily attributed to the transition from one wetland type to another. Long et al. (2021) also investigated wetland dynamics in the Dongting Lake in China using multisource data from 1999 to 2018. To this end, an adaptive-stacking algorithm was developed in GEE, and the results were highly accurate (i.e. the accuracy of change detection was approximately 84%). In another study, Fu et al. (2023) applied different change detection methods to assess the dynamics of mangroves in Beibu Gulf, China. They proposed a novel Detect-Monitor-Predict (DMP) framework for detecting time-series historical changes, monitoring abrupt near-real-time events, and predicting future trends in mangroves. Finally, Fu et al. (2022) investigated the spatio-temporal changes of marshlands and their response to hydro-meteorological factors using the Continuous Change Detection and Classification (CCDC) algorithm applied to optical and Synthetic Aperture Radar (SAR) satellite imagery. They reported that the CCDC algorithm could effectively track the phenology changes of marshes in their study area.

Despite an argument by researchers (e.g. Pasquarella et al., 2022) regarding the limitations of CCDC for non-stationary time series applications, existing literature has demonstrated the applicability of the method in wetland change analysis tasks (DiVittorio et al., 2025; Peng et al., 2021; Wang et al., 2024).

Creating nationally comprehensive baseline data is especially critical in countries like Canada, which harbors a quarter of the world's wetlands (Mirmazloumi et al., 2021). Traditionally, wetland classification has been a laborious and costly endeavor, requiring airborne photography and field visits to conduct wetland surveys. Nonetheless, in Canada, initiatives to map wetlands using satellite imagery have intensified in recent years, resulting in a multitude of scientific research and operational methodologies being employed across diverse geographic areas (Amani et al., 2017; Battaglia et al., 2021; DeLancey et al., 2019; Mahdianpari et al., 2021; Merchant et al., 2020; Montgomery et al., 2021). The advent of GEE has additionally allowed for the processing and analyzing of large datasets covering vast areas and spanning decades, allowing for the assessment of long-term trends.

A large portion of the St. Lawrence Seaway located in Canada is covered by various wetlands. Monitoring the dynamics of these wetlands is of importance to the government of Canada. So far, several studies have discussed wetland change and its reasons in this seaway. For example, Farrell et al. (2010) attributed changes in coastal wetland vegetation communities along the St. Lawrence Seaway to alternations in land use (i.e. agriculture) and water-level regulation. At another site along the St. Lawrence River, Hudon et al. (2005) similarly observed that

wetland vegetation changed significantly with different hydrological regimes related to climate and anthropogenic impacts. Additionally, Dubé et al. (1995) found that logging as a forestry practice, when conducted in forested wetlands within the St. Lawrence lowland, led to a rise in the water table, being a reason for transitions between wetland types or contributed to wetland expansion. Although these studies have discussed wetland changes in the St. Lawrence Seaway, no study has comprehensively investigated the quantitative wetland trends in this region.

As discussed, several studies have already developed the use of remote sensing and machine learning models for mapping and monitoring wetlands in Canada. For example, Amani et al. (2021, 2022) used remotely sensed imagery, machine learning, and big geo data processing models for analyzing wetland changes in Alberta and the Great Lakes from 1984 to 2020. Their results showed that the developed models had a high potential for assessing wetland change in different Canadian ecosystems. Therefore, this study aims to evaluate the previously developed models in the St. Lawrence Seaway and further strengthen the models for an eventual national assessment of wetland change. To this end, 40 years of Landsat archived imagery, along with wetland reference samples, were ingested into an object-based RF algorithm. In total, 12 wetland maps at different time intervals were produced, and then, the trend of wetlands was assessed within GEE. More details are provided in the following subsections.

2. Materials and methods

2.1. Study area

The study area, bounded by the longitudes of −81° and −64°, and latitudes of 44° and 53°, encompasses three drainages surrounding the St. Lawrence Seaway, including Ottawa (146,333 Km^2), St. Lawrence (117,198 Km^2), and portions of North Shore-Gaspe (245,492 Km^2) (Figure 1). These boundaries were extracted from the map of the drainage regions of Canada and confirmed with Natural Resources Canada scientists. The St. Lawrence Seaway extends over 4000 km and encompasses three distinct areas: the Great Lakes (west), the St. Lawrence River (middle), and the St. Lawrence estuary and Gulf of St. Lawrence (east). The middle section of the St. Lawrence River includes the Ottawa and St. Lawrence drainages and is approximately situated between Kingston, Ontario, and Quebec, Quebec. This section is relatively narrower than the estuary and gulf, which includes the North Shore-Gaspé drainage approximately between Quebec, Quebec and the Cabot Straight. The St. Lawrence Seaway was completed in 1959, which connected the natural St. Lawrence River to the Great Lakes through a series of constructed canals and locks. An assessment of wetland changes in the Great Lakes basin was completed by Amani et al. (2022), which is therefore not included in this study.

The St. Lawrence River occupies an old depression that replaced the glacial Champlain Sea during the last glacial period. The region has a diverse geological history, constructed of the Canadian Shield, Appalachian Mountains, and sedimentary platforms, and climate, having temperate, subarctic, and marine influences. As a result, wetlands within the St. Lawrence Seaway drainages range from coastal saline marshes to forested peatlands.

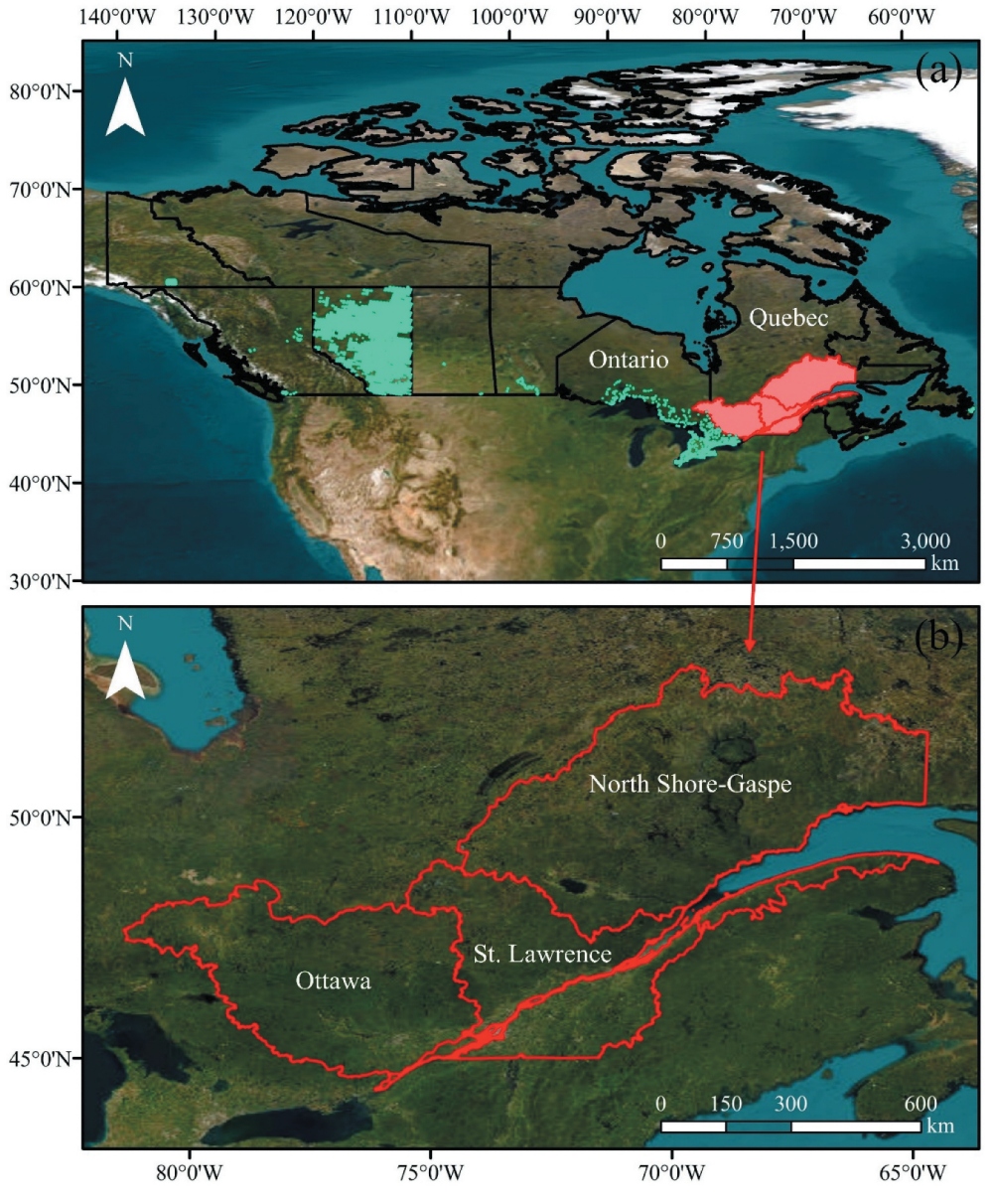

Figure 1. (a) The study area boundaries (red color) within Canada's national boundary (black boundary) and the distribution of the in-situ data (cyan color) Canada. (b) The boundary of the study area (red boundary) for wetland change analysis. The study area includes the three drainages of Ottawa, St. Lawrence, and portions of North Shore-Gaspé.

2.2. Data collection and processing

2.2.1. Reference data

Field data was not available within the study area, and thus, samples were collected from other regions in Canada, such as Alberta and the Great Lakes, which were then employed to train the machine learning models. The reference data were collected by various

organizations over different years, which were then consolidated for further analysis. Figure 1(a) and Table 1 provide the distribution as well as the numbers and areas of the in-situ data, respectively. Figure 2 also illustrates photos of different wetland types along with their Landsat images.

Wetlands were categorized based on the Canadian Wetland Classification System and included Bog, Fen, Marsh, and Swamp (Warner & Rubec, 1997). While Shallow Water (water depth < 2 m) is considered a wetland class, there were not enough Shallow Water samples to accurately train the model. Consequently, all water samples were included in the non-wetland Open Water class.

Identifying non-wetland categories is crucial for obtaining accurate information regarding the location and extent of wetland classes. Without this differentiation, there would be significant confusion between wetland and non-wetland classes. Therefore, five non-wetland classes that are mostly found in the study area were also considered in the classifications and change analysis. The non-wetland classes included the Forest (e.g. deciduous, coniferous, and mixed woodlands), Grassland/Shrubland, Cropland, Barren

Table 1. The numbers and areas of field samples (polygons) for each wetland and non-wetland class.

Class	Total Number*	Area (Km^2)
Bog	3,578 (972)	394.97
Fen	21,454 (5,758)	2,555.75
Marsh	5,557 (521)	358.04
Swamp	19,468 (9,523)	1,466.64
Open Water	4,759 (4,001)	656.26
Forest	89,552 (29,023)	8,413.00
Cropland	9,955 (329)	3,833.94
Grassland/Shrubland	16,043 (2,985)	2,963.49
Barren	760 (720)	288.43

*Values in the parentheses show the number of unchanged samples after applying the Continuous Change Detection and Classification (CCDC) algorithm (see Section 2.3.1).

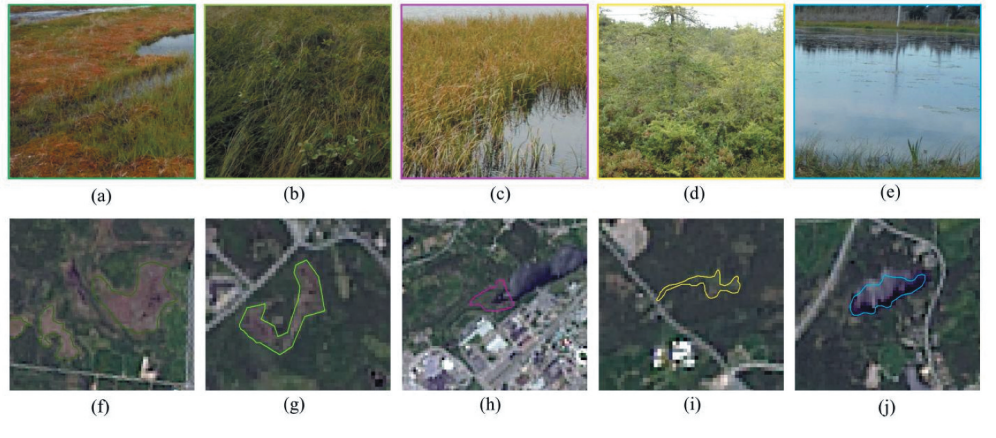

Figure 2. The photos of (a) Bog, (b) Fen, (c) Marsh, (d) Swamp, and (e) Shallow Water. (f)–(j) show these wetland types in the corresponding Landsat images, respectively.

(e.g. urban, rock, bare soil, sand, and other non-vegetated areas), and Open Water (i.e. deep and shallow water bodies).

2.2.2. Satellite data

In this study, archived Landsat satellite images spanning the past four decades were employed through the use of GEE. The imagery captured every two to four years was combined to produce a time series of mosaics for the entire study area. Since the study area experiences significant cloud cover, especially in the northern regions, it was not possible to create cloud-free images within narrower time intervals (i.e. annually). Table 2 provides information on the Landsat data used at different time intervals. In total, 12 mosaic images were produced at different time intervals from 1984 to 2021. These mosaic images were produced by processing 11,650 of Landsat-5/7/8 satellite images.

Initially, cloud, cloud shadow, and snow/ice pixels were masked from all images within GEE. The images were subsequently divided into two groups per interval, categorized by the season of image acquisition (i.e. Spring/Summer: April–July, Summer/Fall: August–October). Winter images (i.e. November–March) were omitted due to snow and high cloud cover. Within each group, all images were then downsampled into a single mosaiced composite by calculating the mean value per pixel in each spectral band over the entire time series (i.e. Spring/Summer and Summer/Fall mosaic images).

2.3. Classification and change analysis

The authors have already developed several advanced wetland classification and change detection models using a variety of satellite datasets, including those collected by Landsat (e.g. Amani et al., 2021, 2022). The classification models were mainly based on an object-based RF algorithm, which typically yields higher accuracy in wetland classification compared to other commonly used machine learning models like Support Vector Machine (SVM) and Maximum Likelihood (ML) (Amani et al., 2017). The change detection models were also based on a combination of different algorithms, such as image and class differencing. Considering the high potential of the previously developed models, the main goal of this study is to investigate the capability of the models to map wetlands over a new study area (i.e. St. Lawrence Seaway in this study). This will subsequently confirm the potential of the developed models for wetland change assessment for the entire

Table 2. Type and number of Landsat images used in each time interval.

Interval number	Interval range	Landsat-5	Landsat-7	Landsat-8	Number of images
T1	1984–1987	×			694
T2	1988–1992	×			872
T3	1993–1996	×			693
T4	1997–2000	×			979
T5	2001–2003	×			1,191
T6	2004–2006	×			1,209
T7*	**2007–2009**	**×**			**1,130**
T8	2010–2012	×			918
T9	2013–2014		×	×	844
T10	2015–2016		×	×	886
T11	2017–2018		×	×	880
T12	2019–2021		×	×	1,354

*The bolded time interval served as the reference period for conducting change analysis.

Canada. Additional details regarding the implemented models are elaborated in the subsequent subsections and publications by Amani et al. (2021, 2022).

2.3.1. Unchanged reference samples selection

As reference samples were not accessible for all periods between 1984 and 2021, a methodology was devised to choose spectrally unchanged reference samples, thereby extending the reference data to cover all 12 time intervals. Initially, all available field samples were subjected to analysis using the CCDC method (Zhu & Woodcock, 2014). This process aimed to select unchanged samples and generate additional field samples for each time interval where corresponding field data was unavailable. The CCDC method accomplishes this selection by scrutinizing all field samples and exclusively choosing those whose spectral responses have remained unchanged throughout the study period (i.e. between 1984 and 2021). The resulting samples, termed unchanged field samples (refer to Table 1), were utilized as training data for all years. In the CCDC method, the field samples were assessed using NDVI $\left(\frac{NIR-Red}{NIR+Red}\right)$, Normalized Difference Water Index $NDWI = \left(\frac{Green-NIR}{Green+NIR}\right)$, and Normalized Difference Build-up Index $\left(NDBI = \frac{SWIR-NIR}{SWIR+NIR}\right)$ calculated from the pre-processed Landsat imagery. The parameterization of the CCDC model in this study followed Amani et al. (2021, 2022). Figure 3 shows CCDC fitting samples for four wetland types, which were categorized as changed and unchanged samples during the process. It is worth noting that discontinuity and significant changes were considered to exclude changed reference samples and ensure having a reliable consolidated reference samples database.

2.3.2. Classification

Object-based approaches have gained favor over pixel-based methods for wetland mapping due to their ability to incorporate multiple data inputs, capture class heterogeneity, and reduce noise (Corcoran et al., 2015; Mahdavi et al., 2018; Montgomery et al., 2021). Previous studies have also shown that integrating various spectral indices, such as NDVI, NDWI, and NDBI, alongside Landsat's spectral bands can enhance classification accuracy (Amani et al., 2017; Zhu & Woodcock, 2014). In this study, the following spectral bands and indices were fed into the Simple Non-Iterative Clustering (SNIC) algorithm in GEE for image segmentation: the blue, green, red, NIR, and SWIR spectral bands, as well as three spectral indices of the NDVI, NDWI, and NDBI. SNIC evenly disperses several seeds across the image, dividing it into numerous superpixels. Pixels are then assigned to clusters based on their distance from the segment centroid, with centroids recalculated until convergence (Achanta & Süsstrunk, 2017). Following SNIC implementation, the segmented image was input into an RF classification algorithm in GEE, chosen due to previous findings suggesting the effectiveness of RF for wetland mapping (Mahdavi et al., 2018). The selection of RF was based on a comparison study for wetland classification in NL, Canada, demonstrating the accurate performance of this machine learning algorithm (Amani et al., 2017). All unchanged samples identified through the CCDC method were utilized to train the RF model for generating wetland maps across different time intervals.

Since there were no field samples from the study area, the accuracies of the classified wetland maps were mainly investigated by visual interpretations. However, later, a wetland ecologist familiar with the St. Lawrence Seaway

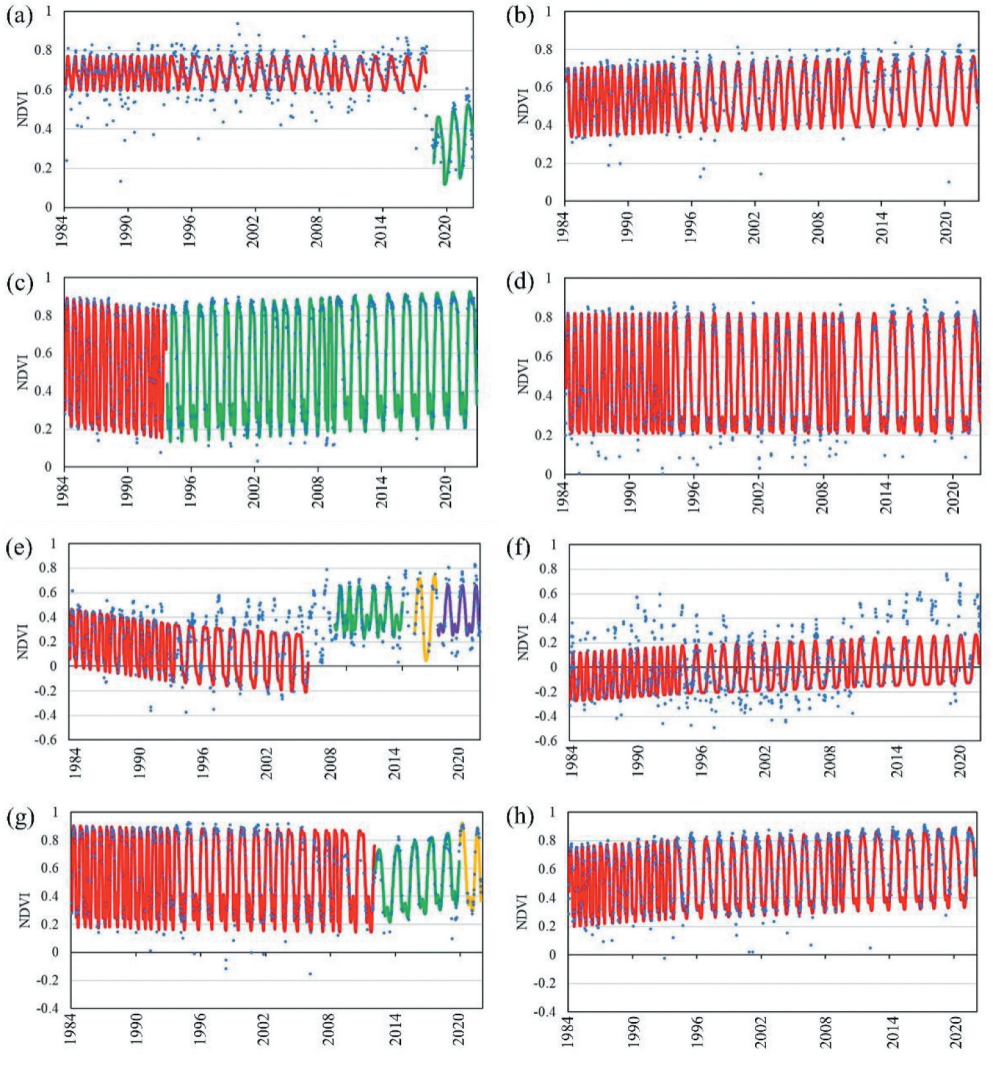

Figure 3. Examples of Continuous Change Detection and Classification (CCDC) fits for four wetland types in the study area respectively identified as changed and unchanged Bog (a, b), Fen (c, d), Marsh (e, f), and Swamp (g, h) based on the time series NDVI values between 1984 and 2021. Left column shows areas where wetlands changed over time and, thus, there are different fits, displayed as various colors. However, right column shows areas where wetlands did not change over time and, therefore, there is only one fit illustrated as one color (i.e. red). Blue points are NDVI values.

generated several reference samples representing different wetland and non-wetland classes through the interpretation of very high-resolution Google Earth imagery. Then, the statistical accuracies of the maps were investigated using the confusion matrix. This was done by calculating several accuracy measures, such as Overall Accuracy (OA), Producer Accuracy (PA), User Accuracy (UA), Omission Error (OE), and Commission Error (CE).

2.3.3. Change detection

After generating the 12 wetland maps, a change analysis was conducted using a combination of object-based class differencing and pixel-based image differencing. This dual approach enhanced the accuracy of the analysis while reducing the overestimation of changed areas and noise, respectively. The object-based analysis involved differencing two object-based wetland maps from consecutive time intervals, while the pixel-based analysis calculated the spectral distance between pixels from two-time intervals using the spectral angle mapper distance. A threshold of 70% was applied to identify changed pixels. The resulting change map was obtained by intersecting the object- and pixel-based analyses. Detailed descriptions of these methods can be found in (Amani et al., 2021, 2022). The outputs of this step were wetland change maps between different time intervals, allowing for spatiotemporal wetland monitoring in the St. Lawrence Seaway region.

3. Results

3.1. Classification

The 12 produced wetland maps were created using the methods described in Section 2.3.2. The map produced for the T7 (2007–2009) (see Figure 4) was selected as the reference interval because it was visually identified as the most accurate wetland map. A visual inspection of all 12 maps demonstrated an overall good alignment with real-world features. For example, Open Water bodies were accurately delineated, and Croplands were concentrated in the southern areas of the study area where agriculture predominantly occurs (i.e. Ottawa and St. Lawrence drainages, as opposed to the northern, forested regions of the North Shore-Gaspé drainage). Peatlands (i.e. fens and bogs) are mostly found in the North Shore-Gaspé area. Some confusions were observed between peatlands and forests in the North Shore-Gaspé area, likely due to the occurrence of wildfire and the altering of the spectral signatures of the sparser canopy cover. For example, a decrease in canopy cover can result in the understory or ground cover providing a greater influence on a site's spectral response and appearing more spectrally similar to fens or bogs. This confusion was not as readily observed in the Ottawa drainage area, where wildfires were less common. Shoreline marshes were also confused with other classes due to the spatial resolution of the Landsat imagery limiting the ability to capture small linear features. Similarly, swamps that form the transition between wetlands and uplands were confused with another wetland or a non-wetland class (e.g. Forest), likely due to the similarity in spectral signatures (i.e. due to similar vegetation) or spatial resolution of the imagery. Nevertheless, overall, it was determined through visual accuracy assessment that all maps exhibited acceptable accuracies for the change analysis.

Since field reference samples of the study area were collected in the latest year of the study by a wetland ecologist, only the confusion matrix of the wetland map was produced for the T12 map (2019–2021) and is provided in Table 3, indicating an overall classification accuracy of 78.2%. Moreover, both the averaged PAs and UAs were approximately 75%, suggesting a satisfactory level of accuracy in discriminating between different wetland and non-wetland classes using Landsat data. Notably, the highest PAs and UAs were observed for the non-wetland classes, particularly Barren, Cropland, and Open Water.

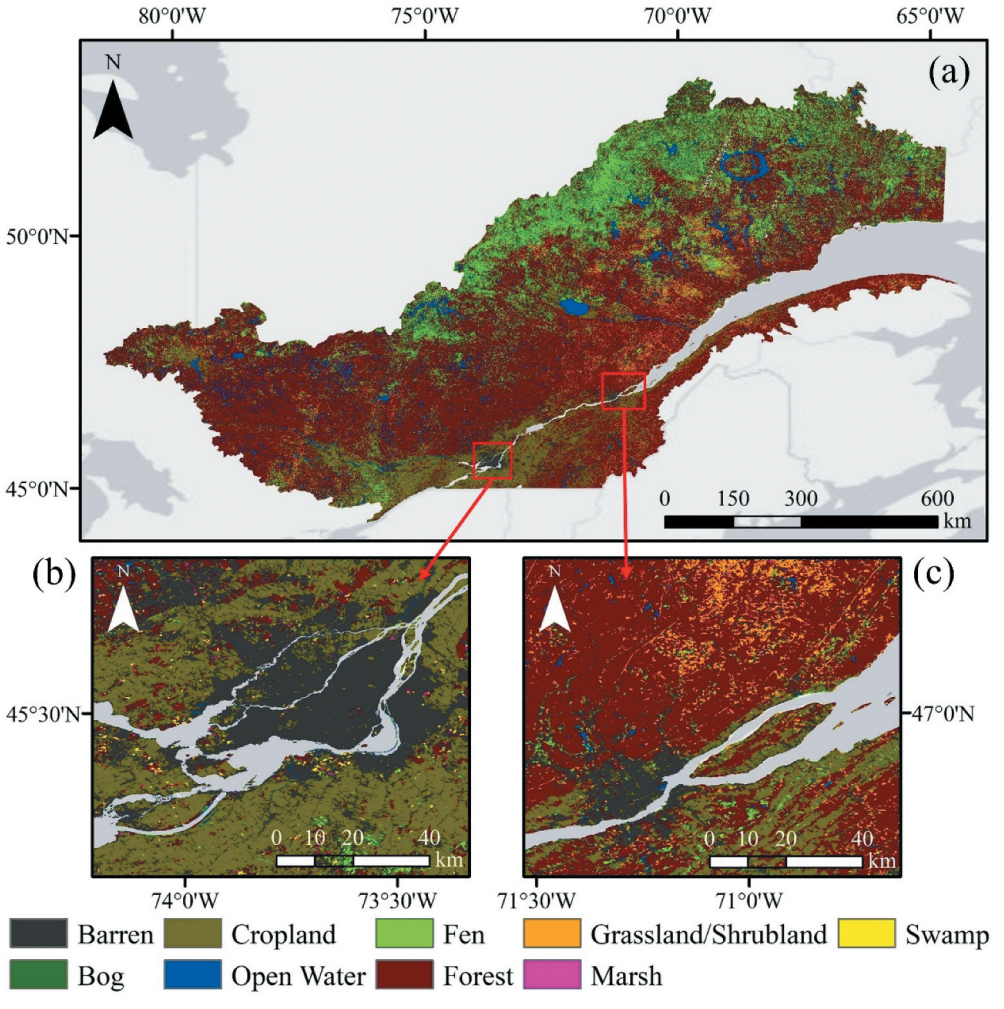

Figure 4. (a) Wetland classification map generated for the reference time interval (2007–2009) from the study area and examples from the (b) Montréal region and (c) Québec City region.

While the class accuracies for the wetland classes were also reasonable, the PAs and UAs for the Fen and Swamp classes ranged between 50% and 61%. The confusion matrix revealed the highest confusions between Bog and Fen, as well as between Swamp and Forest. For instance, 15 pixels out of 108 pixels of Fen were misclassified as Bog, while 35 pixels out of 399 pixels of the Forest class were erroneously identified as Swamp. This can be attributed to the ecological and spectral similarities between Bog and Fen, as well as the inherent difficulty in discriminating between Forest and Swamp classes using solely optical satellite data.

3.2. Change analysis

Several change analyses were performed using the produced wetland maps to assess trends occurring over the study area in the last four decades. However, it is important to

Table 3. The confusion matrix based on the number of pixels for the wetland map of the time interval of 2019–2021 (PA, UA, OE, CE, and OA indicate Producer Accuracy, User Accuracy, Omission Error, Commission Error, Overall Accuracy, respectively).

		Reference Data											
		Barren	Bog	Cropland	Open Water	Fen	Forest	Grassland/ Shrubland	Marsh	Swamp	Total	UA (%)	CE (%)
Classified	Barren	265	3	13	0	4	4	5	0	2	296	89.5	10.5
	Bog	4	82	3	0	15	2	2	8	11	127	64.5	35.5
	Cropland	11	3	320	0	5	3	19	2	9	258	86.0	14.0
	Open Water	0	0	0	169	1	0	0	5	3	178	94.9	5.1
	Fen	3	16	10	0	61	16	8	7	1	122	50.0	50.0
	Forest	5	6	3	0	7	309	10	12	19	371	83.2	16.8
	Grassland/Shrubland	8	1	16	0	8	23	177	10	7	250	70.8	29.2
	Marsh	2	9	5	4	6	7	0	127	6	166	76.5	23.5
	Swamp	6	7	5	2	1	35	11	8	60	135	54.5	45.5
	Total	304	127	261	175	108	399	232	179	118	1,903		
	PA (%)	87.1	64.5	85.3	96.5	56.4	77.4	76.2	70.9	60.8		**OA = 78.2%**	
	OE (%)	12.9	35.5	14.7	3.5	43.6	22.6	23.8	29.1	39.2			

note that while the 12 wetland maps demonstrated good accuracy, any misclassifications or errors in the classification would propagate into the results of any change detection analysis, resulting in additional uncertainties.

3.2.1. Overall change

A change analysis was performed to assess the overall change that occurred between 1984 and 2021. The results indicated that 2.46% (12,495 km^2) of the study area underwent landcover changes, while 98% (495,594 km^2) remained unchanged (Figure 4). The greatest amount of changed areas was observed in the North Shore-Gaspé area (1.46%), with change occurring sporadically throughout the Ottawa (0.58%) and St. Lawrence drainages (0.42%). Change in the Ottawa and St. Lawrence drainages was observed to occur in and around urban and agricultural regions and likely reflects the exposure of wetlands to agriculture and other human pressures. Scientific studies conducted by Environment and Climate Change Canada have estimated that the majority of wetlands in this region lack a buffer zone, making them more susceptible to encroachment. Agriculture and human settlement have occupied the area adjacent to St. Lawrence since the beginning of the colonial period, over which the wetland area has significantly decreased and been altered. The Baie-Comeau region, in the North Shore-Gaspé area, was noted as a change hotspot (Figure 5(c)). However, additional inquiries found that certain observed alterations are connected to either wildfires or industrial activities that have changed the land's covering. This can be due to the bright spectral signature that occurs after the forest canopy has been removed, being confused and mapped as wetland classes. It should also be noted that since wetland maps were not produced without error, and machine learning algorithms, such as the object-based RF used in this study, inherently contain misclassification errors, these errors could propagate into the change detection analysis. However, the observed changes across the study area were not solely attributable to classification errors. Visual assessment of the change results revealed that changed pixels were distributed both within and along the boundaries of various land cover types. For example, wetland areas exhibited both boundary shrinkage and expansion due to water regulations and, in some cases, were converted into other land cover types (e.g. Cropland and Forest) and vice versa.

3.2.2. Change frequency

Figure 6 shows the number of changes that occurred over the changed areas (red areas in Figure 5). This was obtained using 12 time-series wetland maps. Most areas were only changed once (81%) and twice (15%) between 1984 and 2021, and a small portion (3%) of the area was changed three times. In total, only 1% were changed four, five, six, seven, eight, and nine times.

3.2.3. Change trend analysis

A follow-up analysis of changes was performed to evaluate trends between 1984 and 2021 for both wetland and non-wetland categories, as depicted in Figure 7. Over the last four decades, there has been a consistent decline in bog and fen areas, while swamp areas have gradually expanded. Marsh area was relatively unchanged until the 2004–2006 time interval, with a sharp increase in the 2013–2014 time interval. Barren and Cropland areas increased across the four decades, likely at the expense of wetland loss through urban

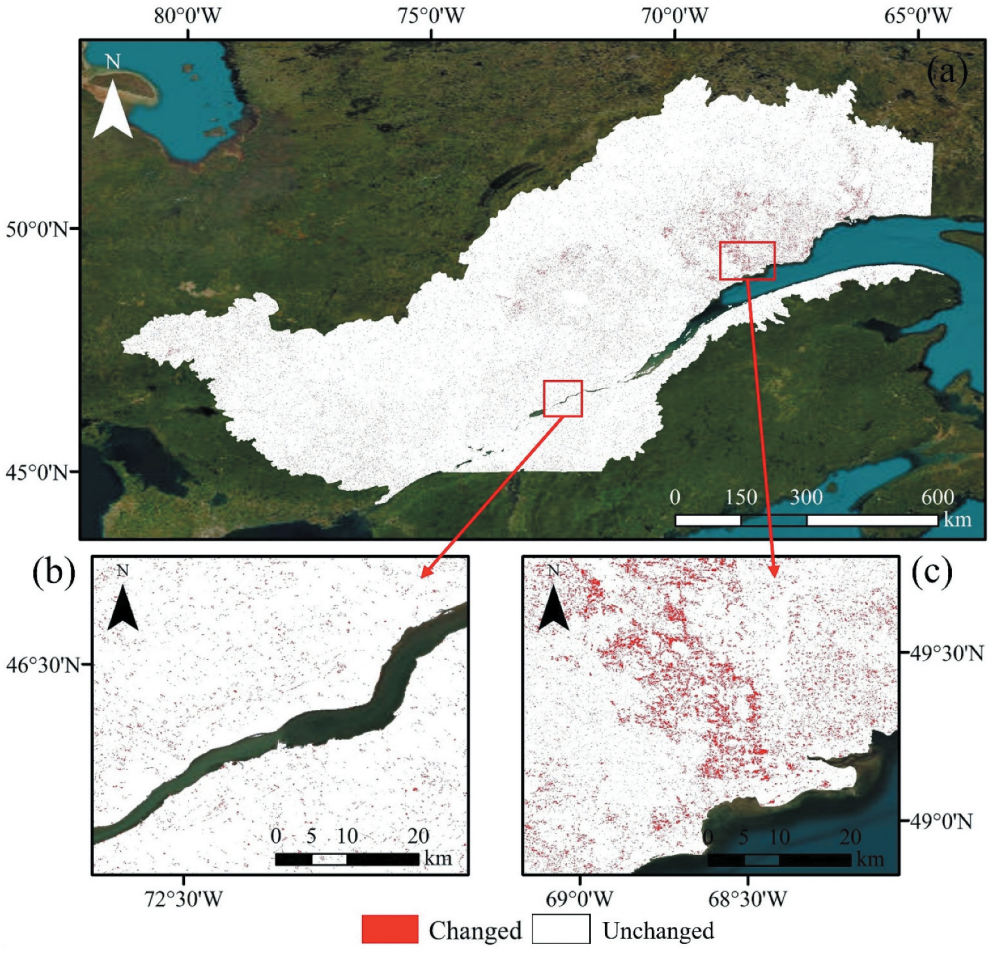

Figure 5. (a) Binary Changed/Unchanged map for the study area and examples from the (b) Trois-rivières region and (c) area surrounding Baie-Comeau.

and agricultural expansion. Forest areas also increased since 1984 but less significantly than Barren and Cropland. Similarly, Grassland/Shrubland area increased consistently until the 2007–2009 time interval, after which it remained stable, though the relative change is small compared to Barren and Cropland. Open Water areas did not vary substantially, and the trend observed is likely related to inter-annual water level variation within the St. Lawrence Seaway. Water levels within the seaway are regulated for hydro-electric and navigational purposes, as well as are influenced by other human activities, such as industry and agriculture. Water level regulation and the encroachment of agri-culture and human settlements may also contribute to the trend observed for Marshes. Marshes were often removed from the landscape for agriculture and are particularly sensitive to fluctuations in water level. In recent decades, there has been a sustained national campaign to conserve, restore, and protect wetlands in the landscape, which has led to the restoration of many wetlands, typically Marshes. Swamps often occur in riparian areas alongside Marshes and may have increased in area for similar reasons.

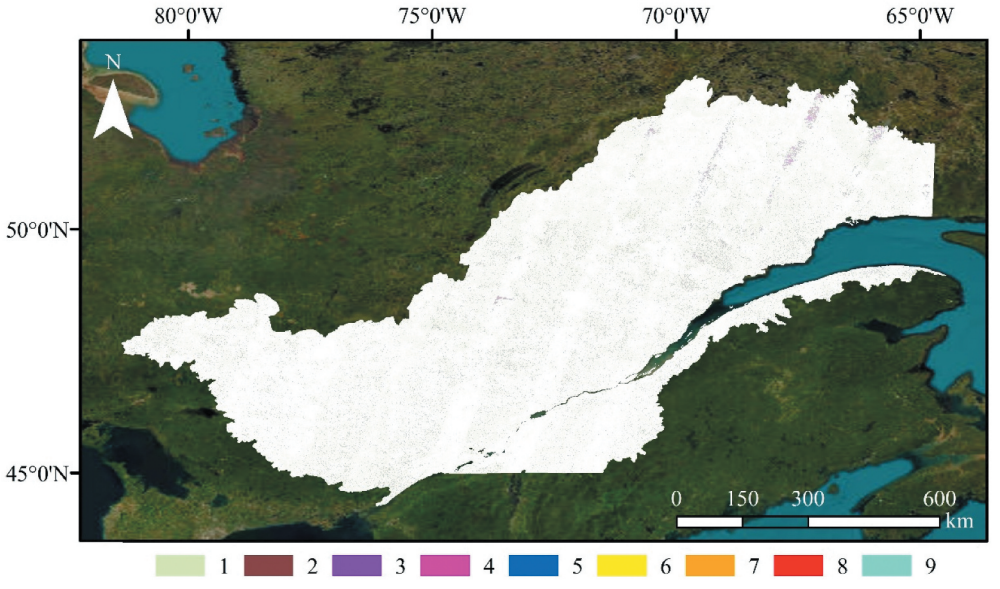

Figure 6. Frequency of changes from 1984 to 2021.

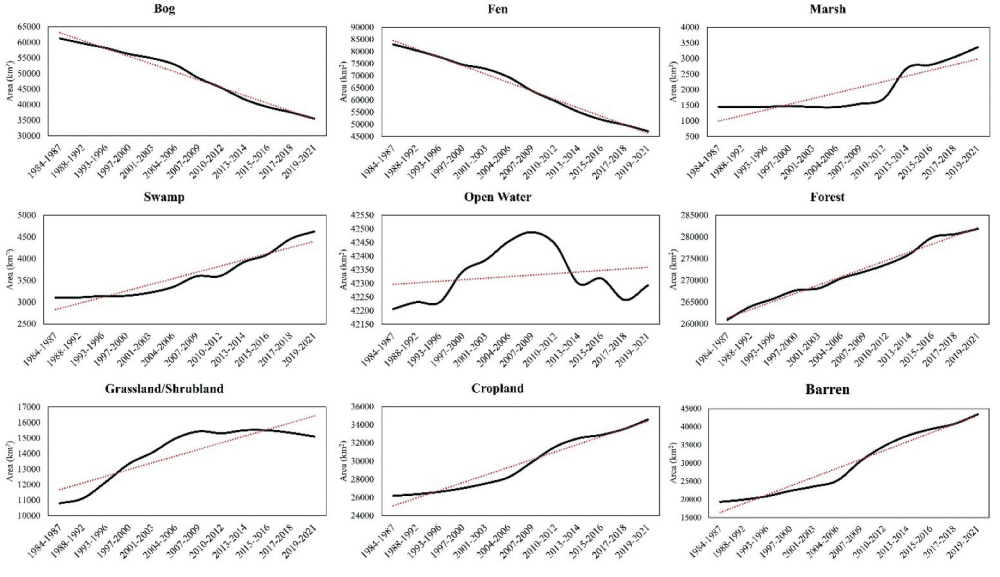

Figure 7. Variation in areas of wetland and non-wetland classes over the past four decades. The dotted red line shows the linear trendline.

3.2.4. Gain and loss

An analysis of changes was carried out to evaluate the increase and decrease in both wetland and non-wetland categories over the last four decades. This was completed by reclassifying the changed/unchanged map (Figure 8) to indicate (a) areas where non-wetlands were converted to wetlands (Gain) and (b) areas where wetlands were

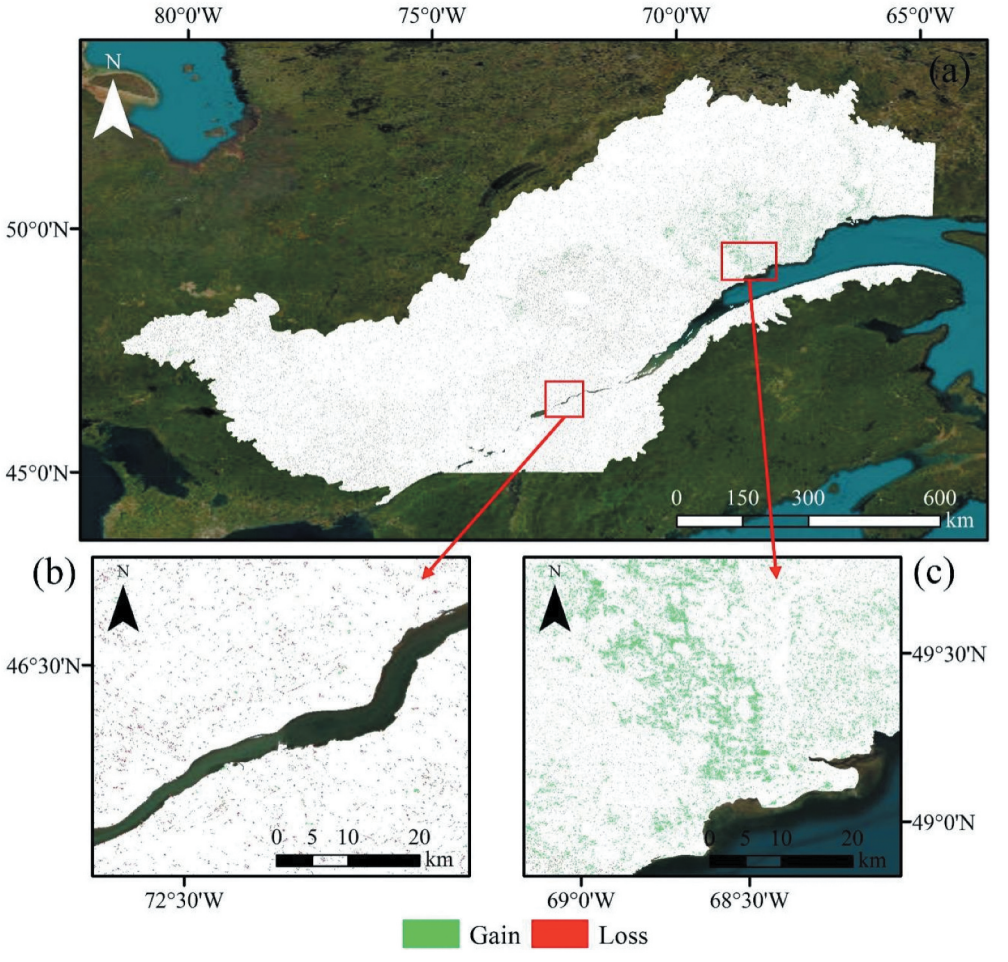

Figure 8. (a) The spatial distribution of wetland gain and loss across the study area and examples from (b) the Trois-Rivières region experiencing primarily wetland loss and (c) the area surrounding Baie-Comeau experiencing primarily wetland gain.

converted to non-wetlands (Loss). The findings revealed a net increase in wetlands within the study area, with 6,793 km^2 of wetland gain identified and 5,701 km^2 lost.

Wetland gain was primarily observed in the North Shore-Gaspé area (1.07% gain and 0.38% loss), with the loss occurring throughout the Ottawa (0.14% gain and 0.44% loss) and St. Lawrence (0.12% gain and 0.30% loss) drainages. Wetland loss did not appear to be associated with one particular cause, such as agricultural or urban expansion, but tended to occur along wetland boundaries, suggesting there has been a decrease in overall wetland size. This may be the result of hydrological changes whereby a decrease in saturated conditions can lead to wetlands being converted to non-wetlands or the increased prevalence of saturated conditions converting wetlands to open water. Additionally, this may reflect the encroachment of human activities. Similarly, wetland gain did not appear directly associated with a particular cause, with gain also observed along wetland boundaries. As previously mentioned, it was noted that some more

expansive areas of mapped wetland gain seemed to be due to changes in forest cover rather than from a change from forest to wetland. This could be due to the loss of forest cover due to wildfire, forestry, or other industrial development, to be incorrectly mapped as wetland classes after the initial period.

3.2.5. Transition between classes

Table 4 shows land cover transitions for nine classes between two time intervals of 1984–1987 and 2019–2021. Based on the results, the most significant change occurred in the Fen class, with an area of 1,552.4 km^2 transitioning into Forest. Although the Barren class did not lose much of its area, several other classes have changed to the Barren class, including 93 km^2 of Bog, 121 km^2 of Fen, and 220 km^2 of Forest classes. Similarly, while a portion of the Bog, Fen, and Forest classes has changed into croplands, the Cropland class did not lose a considerable part of its area. Additionally, a substantial area of both Fen and Forest classes (i.e. 480 km^2 and 946 km^2, respectively) was converted to Grassland/Shrubland. Finally, 1,382 km^2 of Grassland/Shrubland changed to Forest, and most other changes in the areas of the classes were insignificant.

4. Discussion

In this study, the method developed by Amani et al. (2021, 2022) was applied to wetland change analysis in the St. Lawrence Seaway. Despite the satisfactory results, there were multiple specific challenges, which are described below. Moreover, several suggestions are provided for future studies that might be interested in utilizing this cloud computing approach for wetland change detection in other areas.

Since there was no in-situ data from the study area, reference samples were used from other regions. In fact, we assumed that the wetland conditions in the other regions of Canada are similar to those found in the St. Lawrence Seaway. This assumption is correct to a certain degree. However, it is better to collect field data within the boundary of the study area in future studies to tackle this limitation. Furthermore, due to the absence of field data, the accuracy of the generated wetland maps was solely assessed visually, and no statistical accuracy assessment was conducted comprehensively, except for the last time interval (2019–2021). Hence, despite the utilization of advanced machine learning models for wetland mapping, the accuracy of the resulting maps remains uncertain.

Another challenge was related to the availability of reference samples over the past four decades. Therefore, appropriate reference sample migration algorithms (Ghorbanian et al., 2020; Zhu & Woodcock, 2014) must be incorporated to migrate the recent reference samples to earlier years of the study period. These types of algorithms, especially the one used in this study (i.e. CCDC), possess several limitations that can cause errors, which are propagated into classification maps and change detection analyses (Bourgeau-Chavez et al., 2017). First, CCDC is computationally expensive, and thus, even with a high-performance GEE cloud computing platform, it is not possible to use numerous features for unchanged reference samples determination, which can also decrease the efficiency and reliability of the reference sample migration. Second, the CCDC algorithm assumed a simple sinusoidal model to identify unchanged pixels (e.g. reference samples), and thus, complex intra-annual variations in several land cover classes (e.g. Cropland) can also be considered another source of limitation. Finally, since the spectral responses of many

Table 4. The land cover changes (based on km^2) between each pair of classes in the St. Lawrence Seaway between 1994–1987 and 2019–2021 time intervals.

		2019–2021										
		Barren	Bog	Cropland	Open Water	Fen	Forest	Grassland/Shrubland	Marsh	Swamp	Total	Total (%)
1984–1987	Barren	13554.0	0.5	0.4	0.2	0.7	2.2	0.4	0.0	0.0	13558.3	2.7
	Bog	93.3	43529.1	24.3	10.4	4.7	613.5	161.5	9.4	12.9	44459.1	8.8
	Cropland	0.3	0.2	25881.4	0.4	0.3	3.3	1.6	0.1	0.1	25887.7	5.1
	Open Water	12.1	1.5	8.4	38935.6	0.8	57.7	6.4	2.3	1.6	39026.4	7.7
	Fen	121.3	30.7	37.3	32.4	77017.7	1552.4	480.6	25.8	40.5	79338.6	15.6
	Forest	220.0	32.2	89.6	52.5	79.0	279520.7	946.4	49.3	78.9	281068.5	55.3
	Grassland/Shrubland	39.7	8.3	19.6	14.7	27.2	1382.0	15910.7	16.2	19.1	17437.5	3.4
	Marsh	3.6	0.8	3.3	2.7	2.3	102.2	23.7	2234.7	1.9	2375.3	0.5
	Swamp	4.9	0.9	0.9	1.6	2.8	149.5	30.2	2.5	4715.5	4908.7	1.0
	Total	14049.2	43604.1	26065.3	39050.4	77135.4	283383.5	17561.4	2340.3	4870.6	508060.1	100.0
	Total (%)	2.8	8.6	5.1	7.7	15.2	55.8	3.5	0.5	1.0	100.0	

samples have changed over the past 40 years, CCDC does not select them for the classification and change analysis. This fact significantly decreased the sample size for certain categories.

While Landsat data proved to be the most suitable choice for this study's objectives, it is widely acknowledged that combining optical satellite imagery with SAR and Light Detection And Ranging (LiDAR) datasets yields the highest accuracy in wetland classification (Amani et al., 2020; Mahdavi et al., 2018). Therefore, for wetland trend analysis over shorter time spans, integrating open-access optical (such as Landsat and Sentinel-2), SAR (like Sentinel-1 and RADARSAT), and Digital Elevation Model (DEM) datasets can enhance the precision of generated wetland maps and subsequently improve the accuracy of change analysis. Moreover, as discussed in Section 2.2.1, we could produce only 12 cloud-free Landsat mosaics from the study area over the past 40 years, containing two periods of April–July and August–October. The frequency (i.e. number of periods and time intervals) of these images could affect the classification results and, thereby, change analysis results. Overall, it is expected that more mosaic images, both within each period (e.g. seasonal mosaics) and across time intervals (e.g. annual mosaics instead of 12 intervals), would provide more details about wetland classes and changes. For instance, it is believed that the possibility of generating annual mosaic images, resulting in 40 time intervals, would yield more distinctive information for a more robust change analysis. However, due to the consistent cloud cover over the study area, we were restricted to producing only 12 high-quality cloud-free images (12 time intervals) using Landsat archived imagery for the analysis.

In this research, the RF algorithm was utilized for wetland classification. Nonetheless, studies indicate that deep learning models surpass this algorithm in wetland mapping (DeLancey et al., 2019; Mahdianpari et al., 2018; Rezaee et al., 2018). Hence, future investigations could focus on developing advanced deep learning algorithms like Convolutional Neural Networks (CNN) to enhance the accuracy of wetland maps and change detection results. It is worth noting that creating robust and precise deep learning models necessitates a significant volume of training samples.

Various sources of error and limitations, including those previously mentioned, contributed to misclassifications in the generated wetland maps. Consequently, these maps inherently contain misclassification errors that have influenced the subsequent change detection analyses.

Several previous studies have discussed wetland changes in different study areas of Canada (e.g. Mahdianpari et al., 2020). These studies have reported that a large portion of wetlands (10–20%) in the Great Lakes basin, as well as the provinces of Alberta and Newfoundland, were changed throughout the past four decades. These changes were considerably more than the changes observed in this study (i.e. only 2.5%). In fact, the results showed that overall wetland gain was more than wetland loss in the St. Lawrence Seaway. This was most probably because of less anthropogenic activities in the St. Lawrence Seaway compared to Alberta and the Great Lakes, in which there have been significant anthropogenic activities, especially over the past two decades. As described above, further investigations need to be conducted in future studies to explore the reasons behind wetland changes and verify the results of this study. It was also observed that the main wetland changes in Canada were related to the transition between Forest and some of the wetland types, such as Swamp and Fen. This can be

because of (1) deforestation in the country and (2) high confusion between Swamp and Forest in Landsat imagery and the resulting misclassification in the produced wetland maps.

Although the changes in wetlands were obtained in this study, the reasons for these trends (e.g. climate change effects or anthropogenic activities) were not discussed. Wetlands are complex ecosystems that differ from one another and even within the same site due to variations in vegetation, water levels, and chemical conditions influenced by seasons, weather, and disturbances. The ever-changing relationship between wetlands and their surrounding environments can sometimes make wetland features seem different from year to year, even if no actual changes have taken place. Thus, the derived change maps and trends should be investigated further to obtain the cause of these changes.

Although the potential of the proposed method was demonstrated in three large study areas in Canada (i.e. Alberta (Amani et al., 2021), Great Lakes (Amani et al., 2022), and St. Lawrence Seaway in this study), it is required to produce a nation-wide wetland change data to ensure the results can be operationally used for protection of biodiversity and critical habitats, and in climate change mitigation and adaptation efforts. Thus, it is suggested that the models be improved by applying the limitations discussed above and applying them to the entire of Canada to assess the national-wide wetland trends.

5. Conclusion

In this study, remote sensing, machine learning, and cloud computing models were applied to map and monitor wetlands variations within three drainages along the St. Lawrence Seaway, Canada. To achieve this, Landsat archive data available in Google Earth Engine (GEE), dating back to 1984, were utilized to classify both wetland and non-wetland regions. The classification took into account the primary wetland classes found in Canada: Bog, Fen, Marsh, and Swamp, along with five non-wetland classes, to ensure more accurate information regarding the location and extent of wetlands. It was determined that the accuracies of the generated wetland maps at various time intervals were reasonable, considering the intricate nature of wetlands in Canada. The resulting change analysis revealed that approximately 2.46% (12,495 km^2) of the study area had experienced landscape alterations over the past four decades, with the most significant changes observed in the North Shore-Gaspé drainage. There was an overall net gain of wetlands in the study area, with 6,793 km^2 of wetland gain mapped and 5,701 km^2 lost. Over the last four decades, bog and fen areas have consistently declined, whereas swamp area have gradually increased. Marsh area was relatively unchanged until the 2004–2006 time interval, with a sharp increase in the 2013–2014 time interval. The proposed method in this study can help protect and conserve wetlands by providing valuable and up-to-date information about wetlands gain and loss, not only in the St. Lawrence Seaway but also in other regions in Canada.

Disclosure statement

No potential conflict of interest was reported by the author(s).

Notes on contributors

Meisam Amani received the B.Eng. degree in Geomatics Engineering from the University of Tabriz, Tabriz, Iran, in 2012, the M.Eng. degree in Remote Sensing Engineering from K.N. Toosi University of Technology, Tehran, Iran, in 2014, and the Ph.D. degree in Electrical Engineering from Memorial University of Newfoundland, St. John's, NL, Canada, in 2018. He is currently an Earth Observation Research Scientist at Natural Resources Canada. Dr. Amani was an Associate Editor in IEEE JSTARS and the Guest Editor for three special issues in the Remote Sensing journal. He also serves as a regular Reviewer in about 15 international remote sensing journals. He was the recipient of the prestigious Professional Engineers and Geoscientists Newfoundland and Labrador Environmental Award in 2020 due to his contribution to wetland mapping in Canada using advanced machine learning and Big Data processing algorithms. A list of his research works, including over 120 peer-reviewed journal and conference papers, can be found at https://www.researchgate.net/profile/Meisam_Amani3.

Mohammad Kakooei received the B.S., M.Sc., and Ph.D. degrees from the Shahid Beheshti University (SBU), Tehran, Iran, in 2011, the M.Sc. degree from the Iran University of Science and Technology (IUST), Tehran, Iran, in 2014, and the Ph.D. degree from Babol Noshirvani University of Technology (BNUT), Babol, Iran, in 2020, all in electronic engineering. Then he became a Postdoc Researcher with the Department of Computer and Electrical Engineering, BNUT, Babol, Iran. He is currently a Researcher with the Department of Data Science and Artificial Intelligence, Chalmers University of Technology, Gothenburg, Sweden. His skills are not limited to a specific programming language and hardware, and he is qualified in programming from hardware- to software-level systems. He is experienced in programming in MATLAB, C/C++, Python, CUDA, and JavaScript. The implementation platforms vary from local systems to the cloud environment. To support remote sensing big data, he utilized the google earth engine platform in his recent research works considering near real-time earth surface monitoring, urban area analysis, building damage assessment, and wetland and cropland classification. His research interests include image processing, machine learning, remote sensing, parallel processing, GPGPU, and data mining applications.

Rebecca Warren is a methodical and highly organized remote sensing professional with 8 years' experience processing and classifying multispectral, radar, and lidar imagery for large-scale mapping projects. She is proficient with common Geographic Information System (GIS) and image processing software packages, and consistently provides high-quality geospatial products and knowledge to a wide variety of clients. Rebecca has additional field experience in wetland classification, vegetation surveys, and wildlife surveys. Rebecca has played a major role in several satellite-based wetland mapping projects in northwestern Canada, which provided valuable information for land use planning and conservation. She has also provided GIS support for conventional and renewable energy projects in Saudi Arabia and Canada. Along with her geospatial work, Rebecca has conducted vegetation and wildlife surveys, has extensive outdoors experience, and thoroughly enjoys working in the field. Rebecca has collaborated with scientists to research, develop, and implement wetland remote sensing methods and products in varied research initiatives, and is a published peer-reviewed author. She has also given guest lectures on wetland remote sensing at the University of Alberta.

Sahel Mahdavi received the Ph.D. degree in electrical engineering from the Memorial University of Newfoundland, St. John's, Canada, in 2018. She is currently affiliated with the Data Analytics team at Wood Environment and Infrastructure Solutions, Ottawa, ON, Canada. Having almost ten years of academic and industrial background in Remote Sensing, she is familiar with a wide array of topics relevant to RS/GIS and their applications in various environmental aspects. She also coauthored a book entitled Principles of SAR Remote Sensing and has authored more than 40 peer-reviewed journals. Her research interests include object-based wetland classification using a combination of optical and full-polarimetric SAR data, feature selection, soil moisture retrieval using SAR images, image segmentation, speckle reduction in SAR images, target detection in multispectral optical images, and the relationship between environmental conditions and SAR images. Dr. Mahdavi was a member of a provincial project on wetland classification during her Ph.D. when she identified the problem with wetland classification using remote sensing and, subsequently, proposed a novel scheme for wetland mapping. She was the recipient of the Professional Engineers and Geoscientists Newfoundland and Labrador Environmental Award in 2020, the Emera Graduate Scholarship for Distinctive Women in Engineering for three consecutive years (2016–2018), and Newfoundland and Labrador Branch of Canadian Institute of Geomatics Scholarship in 2015.

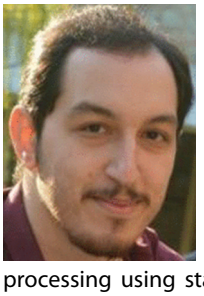

Arsalan Ghorbanian received the B.Sc. degree in geodesy and geomatics engineering, the M.Sc. degree in remote sensing, and a Ph.D. degree in remote sensing from the K. N. Toosi University of Technology, Tehran, Iran, in 2016, 2018, and 2023, respectively. He has worked with different remote sensing datasets during his academic career, including multispectral, hyperspectral, synthetic aperture radar, and thermal infrared data. He has authored or coauthored more than 30 peer-reviewed papers in these fields. His research interests include satellite image (multispectral/SAR/hyperspectral) and video processing using statistical and machine learning methods, land cover mapping, wetlands/mangroves mapping and monitoring, vegetation trend analysis, drought monitoring, sea/ocean studies, and soil moisture estimation. Dr. Ghorbanian has been a regular Reviewer in several international remote sensing journals and is currently a Reviewer Board member of the *Remote Sensing* journal. He has been a Guest Editor for two Special Issues in the *Remote Sensing* journal. He also serves as an Advisory Board member of the *Ecological Indicators*. He was recognized as an excellent student during his B.Sc. and ranked first during his M.Sc. at the K. N. Toosi University of Technology. He was also selected as the Top Researcher in 2022 during his Ph.D. at the K. N. Toosi University of Technology.

Amin Naboureh graduated with a Ph.D. in Physical Geography from the University of Chinese Academy of Sciences (UCAS) in 2022. He works as an Assistant Professor at the Institute of Mountain Hazards and Environment, CAS. His research includes but is not limited to land cover/use mapping, air pollution, drought monitoring, water and agricultural management, and utilizing advanced ML algorithms for environmental management. He has been actively involved in multiple provincial, national, and international projects, serving as both a research team member and a principal investigator. Dr. Naboureh received excellent international student and graduate titles from UCAS in 2021 and 2022, respectively.

Kevin Murnaghan received the Bachelor of Science, Honours Applied Physics, Computer Science minor from the University of Waterloo in 1996. He has been a Remote Sensing Scientist at Natural Resources Canada since 2006 and was a contractor at the Canada Centre for Remote Sensing 1997-2006. Past projects include RADARSAT-1 calibration, airborne SAR 580 calibration and data processing, InSAR for geohazard monitoring, ecological performance mapping of the Yukon River Basin, wetland mapping using radar, and Analysis Ready Data generation for RADARSAT missions.

Data availability statement

The utilized Landsat data are accessible for free download at https://developers.google.com/earth-engine/datasets and https://www.usgs.gov/landsat-missions/landsat-data-access. The GEE code is available upon request from the corresponding author.

References

Achanta, R., & Süsstrunk, S. (2017). Superpixels and polygons using simple non-iterative clustering. *2017 IEEE Conference on Computer Vision and Pattern Recognition (CVPR)* (pp. 4895–4904). https://doi.org/10.1109/CVPR.2017.520

Alonso, A., Muñoz-Carpena, R., Kennedy, E., & Murcia, R. C. (2016). Wetland landscape spatio-temporal degradation dynamics using the New Google Earth Engine Cloud-based platform: Opportunities for non-specialists in remote sensing. *Transactions of the ASABE*, *59*, 1331–1342. https://doi.org/10.13031/trans.59.11608

Amani, M., Ghorbanian, A., Ahmadi, S. A., Kakooei, M., Moghimi, A., Mirmazloumi, S. M., Moghaddam, S. H. A., Mahdavi, S., Ghahremanloo, M., Parsian, S., Wu, Q., & Brisco, B. (2020). Google Earth Engine cloud computing platform for remote sensing big data applications: A comprehensive review. *IEEE Journal of Selected Topics in Applied Earth Observations & Remote Sensing*, *13*, 5326–5350. https://doi.org/10.1109/JSTARS.2020.3021052

Amani, M., Kakooei, M., Ghorbanian, A., Warren, R., Mahdavi, S., Brisco, B., Moghimi, A., Bourgeau-Chavez, L., Toure, S., Paudel, A., Sulaiman, A., & Post, R. (2022). Forty years of wetland status and trends analyses in the great lakes using Landsat archive imagery and Google Earth Engine. *Remote Sensing*, *14*(15), 3778. https://doi.org/10.3390/rs14153778

Amani, M., Mahdavi, S., & Berard, O. (2020). Supervised wetland classification using high spatial resolution optical, SAR, and LiDAR imagery. *Journal of Applied Remote Sensing*, *14*(2), 1. https://doi.org/10.1117/1.jrs.14.024502

Amani, M., Mahdavi, S., Kakooei, M., Ghorbanian, A., Brisco, B., Delancey, E., Toure, S., & Reyes, E. L. (2021). Wetland change analysis in Alberta, Canada using four decades of Landsat imagery. *IEEE Journal of Selected Topics in Applied Earth Observations & Remote Sensing*, *14*(2021), 10314–10335. https://doi.org/10.1109/JSTARS.2021.3110460

Amani, M., Salehi, B., Mahdavi, S., Granger, J. E., Brisco, B., & Hanson, A. (2017). Wetland classification using multi-source and multi-temporal optical remote sensing data in Newfoundland and Labrador, Canada. *Canadian Journal of Remote Sensing*, *43*(4), 360–373. https://doi.org/10.1080/07038992.2017.1346468

Battaglia, M. J., Banks, S., Behnamian, A., Bourgeau-Chavez, L., Brisco, B., Corcoran, J., Chen, Z., Huberty, B., Klassen, J., Knight, J., Morin, P., Murnaghan, K., Pelletier, K., & White, L. (2021). Multi-source EO for dynamic wetland mapping and monitoring in the Great Lakes Basin. *Remote Sensing*, *13*(4), 1–38. https://doi.org/10.3390/rs13040599

Bourgeau-Chavez, L. L., Endres, S., Powell, R., Battaglia, M. J., Benscoter, B., Turetsky, M., Kasischke, E. S., & Banda, E. (2017). Mapping boreal peatland ecosystem types from multitemporal

radar and optical satellite imagery. *Canadian Journal of Forest Research*, *47*(4), 545–559. https://doi.org/10.1139/cjfr-2016-0192

Corcoran, J., Knight, J., Pelletier, K., Rampi, L., & Wang, Y. (2015). The effects of point or polygon based training data on RandomForest classification accuracy of wetlands. *Remote Sensing*, *7*(4), 4002–4025. https://doi.org/10.3390/rs70404002

Davidson, N. C. (2014). How much wetland has the world lost? Long-term and recent trends in global wetland area. *Marine & Freshwater Research*, *65*(10), 934–941. https://doi.org/10.1071/MF14173

DeLancey, E. R., Simms, J. F., Mahdianpari, M., Brisco, B., Mahoney, C., & Kariyeva, J. (2019). Comparing deep learning and shallow learning for large-scale wetland classification in Alberta, Canada. Remote Sensing, *12*(1), 2. https://doi.org/10.3390/rs12010002

DiVittorio, C. A., Wiles, M., Rabby, Y. W., Movahedi, S., Louie, J., Hezrony, L., Cifuentes, E. C., Hinchman, W., & Schluter, A. (2025). Mapping coastal wetland changes from 1985 to 2022 in the US Atlantic and Gulf Coasts using Landsat time series and national wetland inventories. *Remote Sensing Applications: Society & Environment*, *37*, 101392. https://doi.org/10.1016/j.rsase.2024.101392

Dubé, S., Plamondon, A. P., & Rothwell, R. L. (1995). Watering up after clear-cutting on forested wetlands of the St. Lawrence lowland. *Water Resources Research*, *31*(7), 1741–1750. https://doi.org/10.1029/95WR00427

Farrell, J. M., Murry, B. A., Leopold, D. J., Halpern, A., Rippke, M. B., Godwin, K. S., & Hafner, S. D. (2010). Water-level regulation and coastal wetland vegetation in the upper St. Lawrence River: Inferences from historical aerial imagery, seed banks, and Typha dynamics. *Hydrobiologia*, *647*(1), 127–144. https://doi.org/10.1007/s10750-009-0035-z

Fu, B., Lan, F., Yao, H., Qin, J., He, H., Liu, L., Huang, L., Fan, D., & Gao, E. (2022). Spatio-temporal monitoring of marsh vegetation phenology and its response to hydro-meteorological factors using CCDC algorithm with optical and SAR images: In case of Honghe National Nature Reserve, China. *Science of the Total Environment*, *843*, 156990. https://doi.org/10.1016/j.scitotenv.2022.156990

Fu, B., Yao, H., Lan, F., Li, S., Liang, Y., He, H., Jia, M., Wang, Y., & Fan, D. (2023). Collaborative multiple change detection methods for monitoring the spatio-temporal dynamics of mangroves in Beibu Gulf, China. *GIScience & Remote Sensing*, *60*(1), 2202506. https://doi.org/10.1080/15481603.2023.2202506

Ghorbanian, A., Kakooei, M., Amani, M., Mahdavi, S., Mohammadzadeh, A., & Hasanlou, M. (2020). Improved land cover map of Iran using Sentinel imagery within Google Earth Engine and a novel automatic workflow for land cover classification using migrated training samples. *ISPRS Journal of Photogrammetry & Remote Sensing*, *167*, 276–288. https://doi.org/10.1016/J.ISPRSJPRS.2020.07.013

Gorelick, N., Hancher, M., Dixon, M., Ilyushchenko, S., Thau, D., & Moore, R. (2017). Google Earth Engine: Planetary-scale geospatial analysis for everyone. *Remote Sensing of Environment*, *202*, 18–27. https://doi.org/10.1016/j.rse.2017.06.031

Hudon, C., Gagnon, P., Amyot, J.-P., Létourneau, G., Jean, M., Plante, C., Rioux, D., & Deschênes, M. (2005). Historical changes in herbaceous wetland distribution induced by hydrological conditions in Lake Saint-Pierre (St. Lawrence River, Quebec, Canada). *Hydrobiologia*, *539*(1), 205–224. https://doi.org/10.1007/s10750-004-4872-5

Jafarzadeh, H., Mahdianpari, M., Gill, E. W., Brisco, B., & Mohammadimanesh, F. (2022). Remote sensing and machine learning tools to support wetland monitoring: A meta-analysis of three decades of research. *Remote Sensing*, *14*(23), 6104. https://doi.org/10.3390/rs14236104

Long, X., Li, X., Lin, H., & Zhang, M. (2021). Mapping the vegetation distribution and dynamics of a wetland using adaptive-stacking and Google Earth Engine based on multi-source remote sensing data. *International Journal of Applied Earth Observation and Geoinformation*, *102*, 102453. https://doi.org/10.1016/j.jag.2021.102453

Mahdavi, S., Salehi, B., Granger, J., Amani, M., Brisco, B., & Huang, W. (2018). Remote sensing for wetland classification: A comprehensive review. *GIScience & Remote Sensing*, *55*(5), 623–658. https://doi.org/10.1080/15481603.2017.1419602

Mahdianpari, M., Brisco, B., Granger, J., Mohammadimanesh, F., Salehi, B., Homayouni, S., & Bourgeau-Chavez, L. (2021). The third generation of pan-canadian wetland map at 10 m resolution using multisource earth observation data on cloud computing platform. *IEEE Journal of Selected Topics in Applied Earth Observations & Remote Sensing*, *14*, 8789–8803. https://doi.org/10.1109/JSTARS.2021.3105645

Mahdianpari, M., Jafarzadeh, H., Granger, J. E., Mohammadimanesh, F., Brisco, B., Salehi, B., Homayouni, S., & Weng, Q. (2020). A large-scale change monitoring of wetlands using time series Landsat imagery on Google Earth Engine: A case study in Newfoundland. *GIScience & Remote Sensing*, *57*(8), 1102–1124. https://doi.org/10.1080/15481603.2020.1846948

Mahdianpari, M., Salehi, B., Rezaee, M., Mohammadimanesh, F., & Zhang, Y. (2018). Very deep convolutional neural networks for complex land cover mapping using multispectral remote sensing imagery. *Remote Sensing*, *10*(7), 1119. https://doi.org/10.3390/rs10071119

Merchant, M., Haas, C., Schroder, J., Warren, R. K., & Edwards, R. (2020). High-latitude wetland mapping using multidate and multisensor earth observation data: A case study in the Northwest Territories. *Journal of Applied Remote Sensing*, *14*(3), 1–18. https://doi.org/10.1117/1.jrs.14.034511

Mirmazloumi, S. M., Moghimi, A., Ranjgar, B., Mohseni, F., Ghorbanian, A., Ahmadi, S. A., Amani, M., & Brisco, B. (2021). Status and trends of wetland studies in Canada using remote sensing technology with a focus on wetland classification: A bibliographic analysis. *Remote Sensing*, *13*(20), 4025. https://doi.org/10.3390/rs13204025

Mitsch, W. J., & Gosselink, J. G. (2007). *Wetlands* (4th ed.). John Wiley & Sons, Inc.

Montgomery, J., Mahoney, C., Brisco, B., Boychuk, L., Cobbaert, D., & Hopkinson, C. (2021). Remote sensing of wetlands in the prairie pothole region of North America. *Remote Sensing*, *13*(19), 3878. https://doi.org/10.3390/rs13193878

Pasquarella, V. J., Arévalo, P., Bratley, K. H., Bullock, E. L., Gorelick, N., Yang, Z., & Kennedy, R. E. (2022). Demystifying LandTrendr and CCDC temporal segmentation. *International Journal of Applied Earth Observation and Geoinformation*, *110*, 102806. https://doi.org/10.1016/j.jag.2022.102806

Peng, J., Liu, S., Lu, W., Liu, M., Feng, S., & Cong, P. (2021). Continuous change mapping to understand wetland quantity and quality evolution and driving forces: A case study in the Liao River estuary from 1986 to 2018. *Remote Sensing*, *13*(23), 4900. https://doi.org/10.3390/rs13234900

Rezaee, M., Mahdianpari, M., Zhang, Y., & Salehi, B. (2018). Deep convolutional neural network for complex wetland classification using optical remote sensing imagery. *IEEE Journal of Selected Topics in Applied Earth Observations & Remote Sensing*, *11*(9), 3030–3039. https://doi.org/10.1109/JSTARS.2018.2846178

Tamiminia, H., Salehi, B., Mahdianpari, M., Quackenbush, L., Adeli, S., & Brisco, B. (2020). Google Earth Engine for geo-big data applications: A meta-analysis and systematic review. *ISPRS Journal of Photogrammetry & Remote Sensing*, *164*, 152–170. https://doi.org/10.1016/j.isprsjprs.2020.04.001

Tang, Z., Li, Y., Gu, Y., Jiang, W., Xue, Y., Hu, Q., LaGrange, T., Bishop, A., Drahota, J., & Li, R. (2016). Assessing Nebraska playa wetland inundation status during 1985–2015 using Landsat data and Google Earth Engine. *Environmental Monitoring and Assessment*, *188*(12), 654. https://doi.org/10.1007/s10661-016-5664-x

Wang, M., Mao, D., Wang, Y., Li, H., Zhen, J., Xiang, H., Ren, Y., Jia, M., Song, K., & Wang, Z. (2024). Interannual changes of urban wetlands in China's major cities from 1985 to 2022. *ISPRS Journal of Photogrammetry & Remote Sensing*, *209*, 383–397. https://doi.org/10.1016/j.isprsjprs.2024.02.011

Warner, B. G., & Rubec, C. D. A. (Eds.). (1997). *The Canadian Wetland Classification System. Canada committee on ecological (biophysical) land Classification*. National Wetlands Working Group, Wetlands Research Branch, University of Waterloo.

Zhu, Z., & Woodcock, C. E. (2014). Continuous change detection and classification of land cover using all available Landsat data. *Remote Sensing of Environment*, *144*, 152–171. https://doi.org/10.1016/j.rse.2014.01.011